

引用格式: SUN Mengru, JI Haiying, XIONG Hao, et al. Generation of Stretched Pulse with Hundred-femtosecond Pulse Widths Based on Multimode-fiber Interference Effect[J]. Acta Photonica Sinica, 2022, 51(2):0251212

孙梦茹, 纪海莹, 熊浩, 等. 基于多模光纤干涉效应的百飞秒展宽脉冲产生[J]. 光子学报, 2022, 51(2):0251212

基于多模光纤干涉效应的百飞秒展宽脉冲产生

孙梦茹^{1,2}, 纪海莹^{1,2}, 熊浩^{1,2}, 洪瑶¹, 马万卓^{1,2}, 王天枢^{1,2}

(1 长春理工大学 空间光电技术国家与地方联合工程研究中心, 长春 130022)

(2 长春理工大学 光电工程学院, 长春 130022)

摘 要: 设计了基于多模干涉效应锁模的掺铒光纤激光器, 利用渐变折射率多模光纤实现了锁模脉冲输出。通过控制泵浦功率, 调节腔内偏振控制器, 实验获得中心波长为 1 528 nm 的展宽脉冲, 3 dB 带宽为 37.2 nm, 脉冲宽度为 973.2 fs。在腔外进行色散补偿, 将展宽脉冲的脉冲宽度压缩至 280.1 fs。此外, 通过提高总泵浦功率至 961.1 mW 并微调偏振控制器, 获得了色散管理孤子分子脉冲输出, 调制周期为 0.32 nm, 对应的脉冲间隔为 24.1 ps。实验采用多模光纤内置在偏振控制器中的锁模结构, 突破了对多模光纤长度的限制, 激光器结构紧凑, 具有出色的稳定性。

关键词: 光纤激光器; 近红外; 多模干涉; 展宽脉冲; 色散管理孤子分子

中图分类号: TN248

文献标识码: A

doi: 10.3788/gzxb20225102.0251212

0 引言

超快光纤激光因在智能制造、通信、光谱探测以及生物医疗等领域具有潜在的应用而受到广泛关注。常用于产生超短脉冲的被动锁模方法包括非线性偏振旋转(Nonlinear Polarization Rotation, NPR)、非线性环形镜(Nonlinear Optical Loop Mirror, NOLM)和非线性放大环形镜(Nonlinear Amplified Loop Mirror, NALM)等, 这些方法结构简单易于搭建, 但对温度、振动特别敏感, 易受到外界环境的影响, 不利于实现稳定的锁模脉冲。另外, 还可以借助半导体可饱和吸收镜、石墨烯以及单壁碳纳米管(Carbon Nanotubes, CNT)等可饱和吸收材料被动锁模获得超短脉冲, 这些材料具有造价低、恢复时间短、损伤阈值高等优点, 但其可饱和吸收特性无法保持长时间稳定。近年来, 基于非线性多模干涉(Multi-Mode Interference, MMI)效应锁模产生超短脉冲的方法引起人们的关注^[1]。与传统锁模器件相比, 该方法具有损伤阈值高、结构简单、光学特性易于控制、波长可调 and 调制深度可控等优点, 可以实现包括传统孤子^[2-4]、耗散孤子^[5-7]、耗散孤子共振^[8]、类噪声脉冲^[9]、展宽脉冲在内的不同类型锁模脉冲。其中, 展宽脉冲光纤激光器能够使脉冲在激光腔内周期性的展宽压缩, 减弱高能量脉冲在光纤中传输的非线性效应, 实现更窄脉宽的超短脉冲, 受到研究者的广泛关注和研究。

通过向激光腔内引入色散补偿光纤、具有正色散的增益光纤、Martinez 结构、啁啾布拉格光纤光栅、高数值孔径光纤等色散补偿器件, 利用 NPR^[10]、NOLM^[11]、CNT^[12] 等常规锁模方式的展宽脉冲锁模光纤激光器得到了充分的研究, 可以实现稳定输出的飞秒脉冲。2018 年 ZHAO F 等将阶跃折射率多模光纤(Multi-Mode Fiber, MMF)和渐变折射率多模光纤(Graded-Index Multi-Mode Fiber, GIMF)熔接在一起, 将混合单模(Single-Mode Fiber, SMF)-多模-单模(SMF-MMF-SMF, SMS)结构作为可饱和吸收体搭建了被动锁模光纤激光器, 实现传统孤子脉冲和展宽脉冲输出^[13]。2019 年, CHEN G 等采用非线性多模干涉锁模结构观察到传统孤子脉冲和展宽脉冲共存的现象, 并进行了原理仿真^[14]。由于非线性多模干涉效应光纤激光器

基金项目: 国家自然科学基金(Nos.61975021, 62005024), 吉林省自然科学基金(No. 20190201271JC), 教育厅项目(No. JJKH20210816KJ)

第一作者: 孙梦茹(1993—), 女, 硕士研究生, 主要研究方向为超快锁模光纤激光器。Email: 2019100204@mails.cust.edu.cn

导师(通讯作者): 王天枢(1975—), 男, 教授, 博士, 主要研究方向为空间光通信、光纤激光器。Email: wangts@cust.edu.cn

收稿日期: 2021-08-09; 录用日期: 2021-10-28

<http://www.photon.ac.cn>

在光纤通信、光纤传感、波分复用等技术中的应用前景广阔^[15],近年来涌现了大量的实验研究。然而,关于在多模干涉效应光纤激光器中展宽脉冲及色散管理孤子分子的报道相对较少,因此开展相关研究将有助于进一步理解多模干涉效应的非线性光学理论。

本文设计了一种工作在近零负色散区的锁模掺铒光纤激光器,基于多模干涉效应实现锁模脉冲输出。通过调节旋转挤压式偏振控制器(Polarization Controller,PC)来改变渐变折射率多模光纤内激光的偏振状态,获得的展宽脉冲宽度为973.2 fs,并可经过腔外压缩至280.1 fs,通过调节PC获得了光谱调制周期为0.32 nm的色散管理孤子分子,可为多模干涉光纤激光器的研究提供参考。

1 实验结构

基于SMS结构的色散管理全光纤激光器的实验结构如图1。以一段长0.8 m的单模高掺杂掺铒光纤(Highly Erbium-doped Fiber, HEDF, Er80-8/125, Nurfren)作为增益介质,两个980 nm半导体激光器(Pump1功率350 mW, Pump2功率1W)通过980/1 550 nm波分复用器(Wavelength Division Multiplexer, WDM)将泵浦光耦合至腔内,偏振无关隔离器确保环形腔内光的单向传输。腔内基于SMS结构的类可饱和吸收体(Saturable Absorber, SA)作为锁模器件,其中长0.153 m的渐变折射率多模光纤(GIMF, GI50/125 μm , YOFC)被内置在PC中,通过调节PC来改变多模光纤中光的偏振状态,引入相位差从而实现锁模。使用一段色散补偿光纤(Dispersion Compensating Fiber, DCF)来控制环形腔内的色散。在实验中,DCF的长度为0.3 m,考虑到所有组件的尾纤,总腔长为7.4 m。HEDF、SMF和DCF的群速度色散分别为15.7、18、 -152.6 ps/nm \cdot km。由于GIMF长度远小于单模光纤的长度,GIMF中的多模色散的作用可忽略不计。因此,计算可得腔内净色散为 -0.105 09 ps²,激光器工作在近零负色散区。采用10:90的光耦合器的10%端口将环形腔中激光输出到腔外,剩余的90%用作腔内反馈。腔外采用色散补偿进一步压缩脉宽,并在放大器之前放置一个偏振控制器用于优化脉冲的偏振状态,为了避免功率放大过程中过高的峰值功率导致脉冲的分裂和畸变,在PC和放大器之间熔接了一段DCF预先将脉冲展宽。作为放大结构增益介质的同时,在1 550 nm工作在正常色散的高掺杂掺铒光纤也作为色散补偿的一部分,放大器引入的色散进一步降低了脉冲的啁啾。实验中,输出脉冲的光谱由光谱分析仪(Yokogawa, AQ6375B)测量。时域脉冲首先由带宽为10 GHz的1.5 μm 光电探测器检测,然后由带宽为2.5 GHz的示波器(Agilent, DSO9254A)观测。此外,脉冲的射频频谱信号由频谱分析仪(Agilent N1996A)观测。最后,通过自相关仪(FR-103XL, Femtochrome)对锁模脉冲的脉冲宽度进行测量。

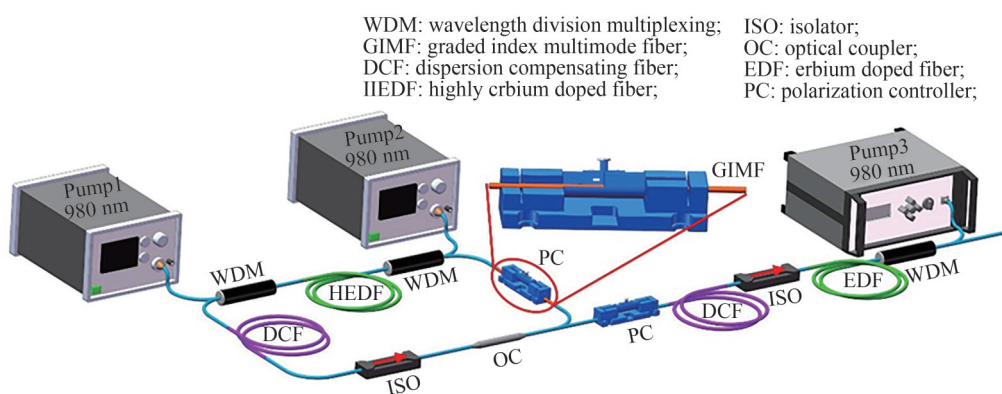


图1 基于SMS结构的色散管理全光纤激光器结构

Fig.1 Structural diagram of SMS structure based dispersion-managed all-fiber laser

基于SMS结构的类可饱和吸收体的示意如图2(a)。其中光束从SMF1注入MMF,并耦合到另一端SMF2中。在忽略模式转换的情况下,来自SMF1的入射光传输到GIMF后激发出高阶模^[16-17]并沿多模光纤传输,在多模光纤内任意位置的光场为所有模式的线性叠加,则在某一特定距离 $z_m(\lambda)$ 处光场与入射光场相同,这就是多模干涉的自成像现象。为了实现超短脉冲锁模状态,GIMF的长度 L_{GIMF} 可设置为

$\left[\frac{(2m+1)}{2} \right] z_m(\lambda)$, m 为整数。此时高功率的光束比低功率的光束透过率大,该结构就能实现类可饱和吸收体的功能^[18]。

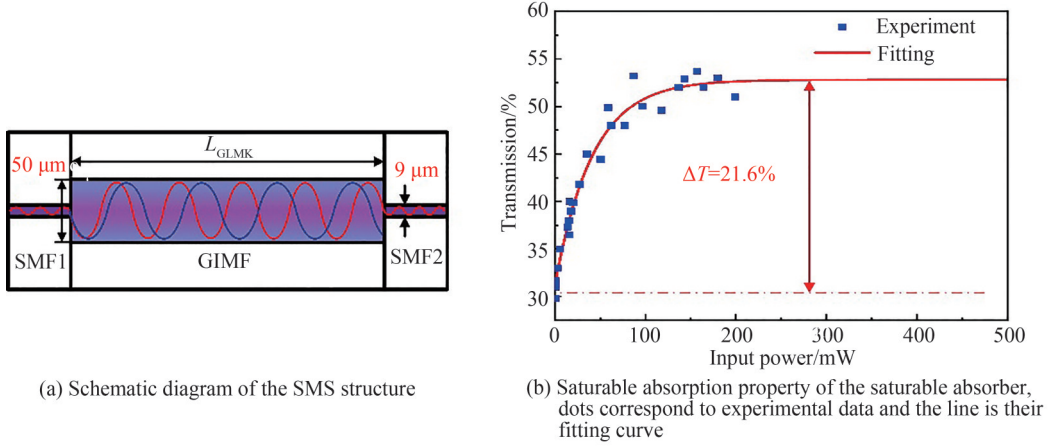


图2 SMS结构示意图及可饱和吸收特性

Fig.2 Schematic and saturable absorption property of SMS structure

实际上,要借助SMS结构实现锁模,GIMF的长度需要控制在微米量级^[19],这无疑增大了该结构的熔接难度。为了放宽对GIMF长度的限制,将SMS结构中的GIMF内置到偏振控制器中。通过调节PC,引入了额外的相移 $\Delta\phi_{NL}$ ^[20-22],并通过调节PC来控制相移的大小。因此,引入的附加相移 $\Delta\phi_{NL}$ 和原始相移 $\Delta\beta_n L_{GIMF}$ 满足

$$\Delta\beta_n L_{GIMF} + \Delta\phi_{NL} = \frac{2m+1}{2} \pi \quad (1)$$

则GIMF的相应长度可表示为

$$L_{GIMF} = \left(\frac{2m+1}{2} - \frac{\Delta\phi_{NL}}{2\pi} \right) \frac{\lambda}{\Delta n_{eff,n}(I)} \quad (2)$$

式中, $\Delta n_{eff,n}(I)$ 为光纤的有效折射率与光强 I 有关。式(1)和(2)表明,由双折射引起的非线性相移将改变所有模式之间的相位差,这一方法放宽了SMS结构对GIMF长度的限制。为了测量SMS结构的可饱和吸收特性,采用一个平衡双探测测量系统^[23],测量结果用式(3)进行拟合,即

$$T = 1 - \Delta T \times \exp\left(-\frac{I}{I_{sat}}\right) - \alpha_{ns} \quad (3)$$

式中, T 为透射率, ΔT 为调制深度, I 为输入光强, I_{sat} 为饱和光强, α_{ns} 为不饱和损耗。调制深度拟合数值为21.6%,如图2(b)所示。

2 结果分析

实验中使用的GIMF光纤的模场直径为50 μm ,与SMF的模场直径9 μm 以及HEDF的模场直径8 μm 均相差很大,光纤间存在一定的熔接损耗。由于激光器需要确保谐振腔内增益与损耗达到平衡才能实现锁模并保持稳定运行,因此激光器的锁模阈值较高。首先固定泵浦2功率,调节泵浦1功率,激光器一直处于连续光工作状态,然后固定泵浦1的功率为95.1 mW,将泵浦2的功率增加至350 mW并调节PC,激光器进入锁模工作状态。由于激光器谐振腔是由正色散光纤和负色散光纤组成的周期性色散管理系统,脉冲在光纤中传输会经历周期性的展宽和压缩。在正色散区域,脉冲积累了大量的正啁啾而展宽,随后进入负色散区域,脉冲的正啁啾得到合适的补偿,脉冲得到压缩,在这种“呼吸”的过程中,脉冲避免了过多非线性相移的积累,经过多次循环后输出展宽脉冲。泵浦2的功率增加至750 mW时锁模脉冲的输出特性如图3。图3(a)为展宽脉冲的光谱,脉冲的中心波长和3 dB带宽分别为1 528 nm和37.2 nm。图3(b)为示波器上实时观察的脉冲序列,脉冲幅度平稳且相邻脉冲间隔为37.03 ns。图3(c)为频谱分析仪测量的射频频谱,脉冲

的信噪比优于 52 dB。采用 1 kHz 分辨率测量的基本重复频率为 27.02 MHz, 对应 7.4 m 的腔长。图 3(c) 中插图 of 采用 5 kHz 分辨率测量的 500 MHz 范围频谱信息, 大范围的射频频谱没有发生调制, 表明激光器运行稳定。测得的自相关迹如图 3(d), 脉冲宽度为 973.2 fs, 对应的时间带宽积 (Time-Bandwidth Product, TBP) 为 4.65, 高于高斯形脉冲的极限变换值, 表明脉冲存在高度的啁啾。脉冲的啁啾是由光纤的高阶色散和模式色散效应引起的, 可以利用适当长度的光纤作为色散延时线进行外部补偿, 实现脉冲宽度压缩。

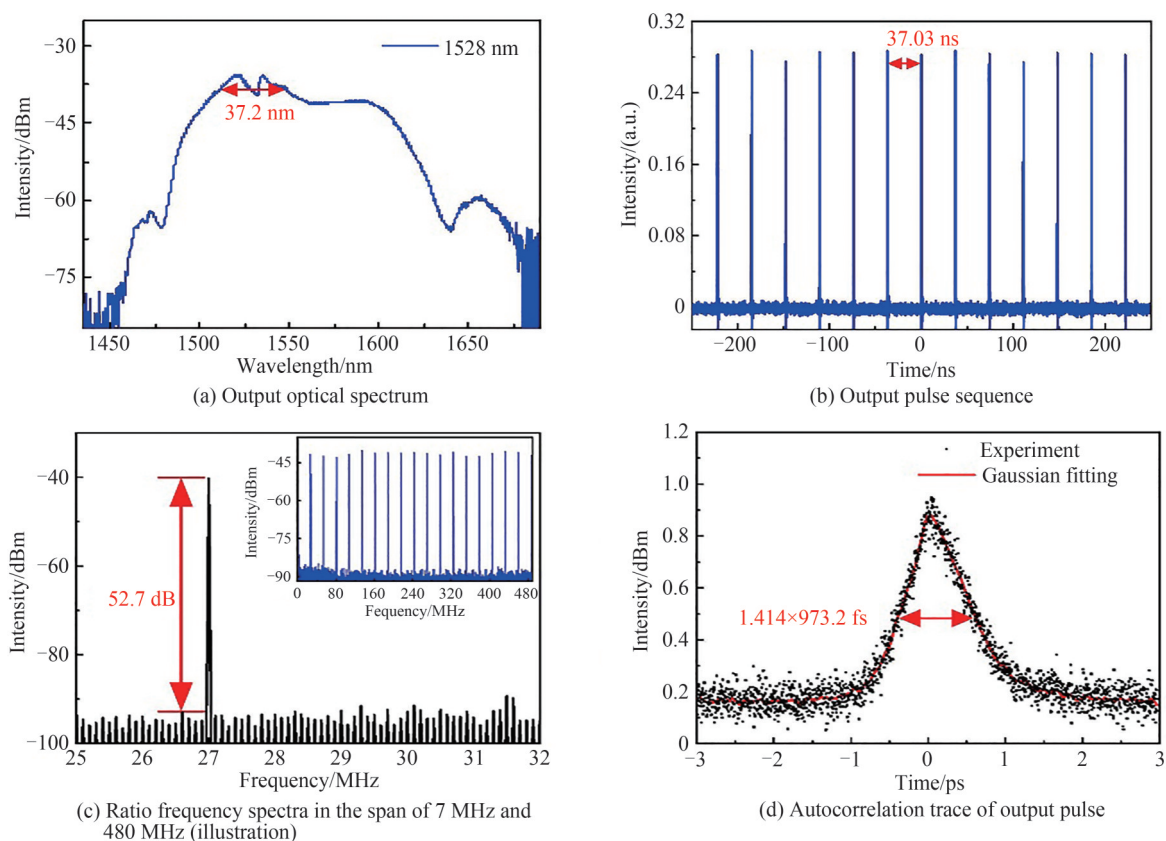


图3 展宽脉冲的输出特性

Fig.3 Output characteristics of the stretched pulse

保持泵浦 1 功率不变, 以 100 mW 的间隔将泵浦 2 功率从 350 mW 增加至 950 mW, 记录每一次功率变化时的输出光谱, 展宽脉冲光谱随泵浦功率的演变如图 4。从图中可知, 光谱的 3 dB 带宽随泵浦功率的增加而逐渐变宽, 3 dB 带宽最大为 37.2 nm。同时, 随着泵浦功率的增加, 谐振腔的净增益增强, 光谱分量的强度显著增加。图 4(b) 为输出功率与泵浦功率的关系, 由于激光器中各部分光纤的熔接损耗较大, 在泵浦 2 功率为 950 mW 时, 谐振腔的最大输出功率为 1.7 mW。

为了获得更窄的展宽脉冲, 在腔外对输出脉冲的脉冲宽度进行压缩。由于 DCF 在 1.5 μm 具有较大的正二阶色散系数, 因此采用回切法来测试不同长度 DCF 的压缩效果, 实验结果如图 5。从图中可知, 随着 DCF 长度增加, 光谱的带宽逐渐增加, 当 DCF 长度为 1.13 m 时, 光谱的 3 dB 带宽达到最大为 38.5 nm。相应的脉冲宽度演变如图 5(b), 脉冲宽度最小能被压缩至 280.1 fs, 此时的 TBP 为 2.01。在功率放大的过程中, 引入的某些非线性啁啾不能被色散补偿抵消, 导致压缩后的实际脉宽与理论转换极限脉宽之间仍存在一定的差距。

为了检测光纤激光器工作的稳定性, 对该激光器的输出光谱和输出功率进行 1 h 连续监测, 每隔 10 min 记录一次输出脉冲的光谱和输出功率。由图 6(a) 可知, 光谱的形状基本保持不变, 激光发射过程中的模式竞争和外界环境的影响导致脉冲的输出特性发生漂移, 中心波长和光谱带宽有轻微的改变。输出功率的波动如图 6(b), 功率抖动小于 ± 0.01 mW。平均输出功率和谱宽均保持相对稳定, 说明激光器具有良好的稳定性。

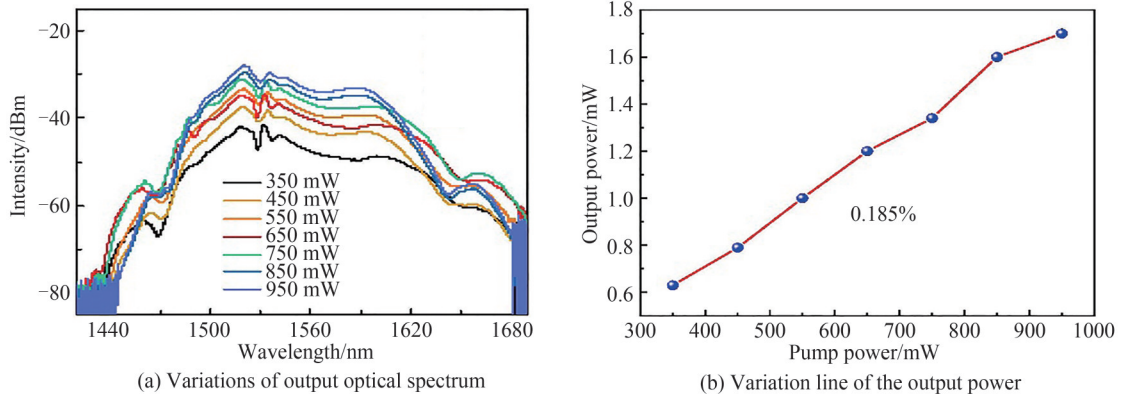


图4 光谱和输出功率随泵浦功率的变化

Fig.4 Variations of the optical spectrum and output power

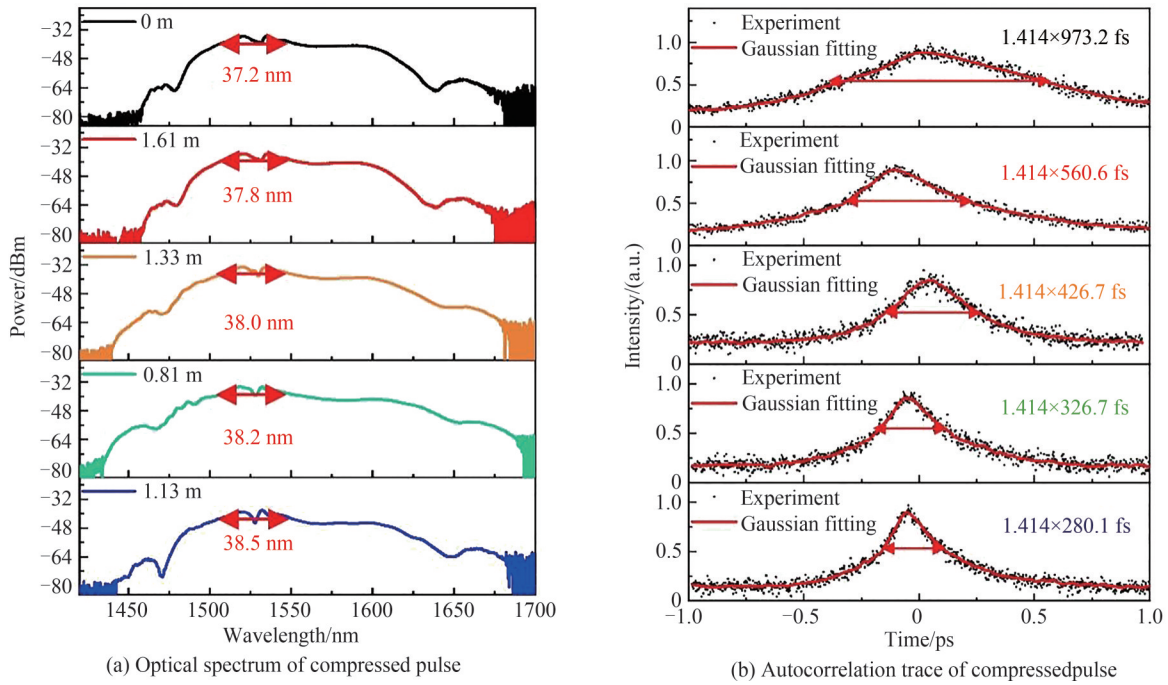


图5 脉冲压缩实验结果

Fig.5 Experimental results of pulse-compression

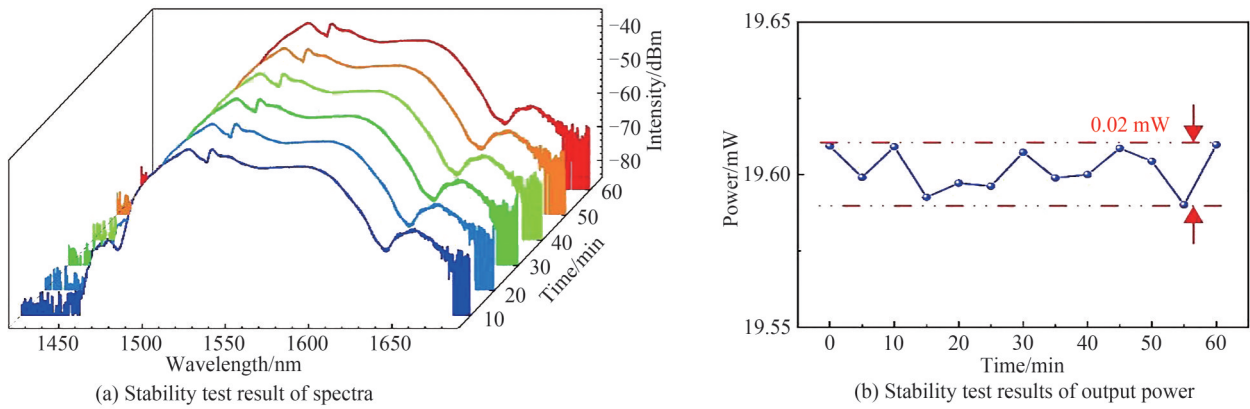


图6 展宽脉冲稳定性测试结果

Fig.6 Stability test results of stretched pulse

在腔内形成稳定的展宽脉冲后继续增加泵浦功率,锁模脉冲的峰值功率受到峰值功率钳制效应的影响不会无限增加,此后继续增大泵浦功率将放大腔内的色散波等背景噪声^[24]。当脉冲的峰值功率足够大时,光纤激光器的工作区域就在正负反馈之间转变。损耗和强度依赖与非线性多模干涉效应之间的动态平衡,使背景噪声(例如色散波)在腔中逐渐生成。由于调制的不稳定性,在腔中产生了背景噪声,脉冲和背景噪声共同作用产生新脉冲。在SMS锁模结构中,通过适当的调节PC可以使得特定频率的背景噪声满足式(2),从而使其在腔内经过循环增益放大后形成新的孤子脉冲^[25]。由于孤子脉冲具有相同的激光增益,孤子间的增益竞争导致孤子能量量子化效应,因此所有的孤子脉冲具有完全相同的参数,随后由于脉冲间吸引力与排斥力的相互作用形成稳定的孤子分子^[26-27]。保持泵浦1功率不变,将泵浦2功率增加856 mW,调节偏振控制器使腔内的偏振态发生改变,脉冲间引力与斥力的弱相互作用导致形成色散管理孤子分子。色散管理孤子分子的输出特性如图7,输出光谱上存在有明显的调制条纹,单个色散管理孤子分子的脉冲宽度为4.04 ps,脉冲间隔为24.1 ps,对应0.32 nm的光谱调制周期。由于脉冲间隔约为脉冲宽度的约6倍,因此该孤子分子脉冲处于松散束缚状态^[28]。图7(b)为自相关迹,自相关迹中三个峰的峰峰比为1:3:1,束缚态脉冲具有相同的脉冲宽度和固定的时间间隔。

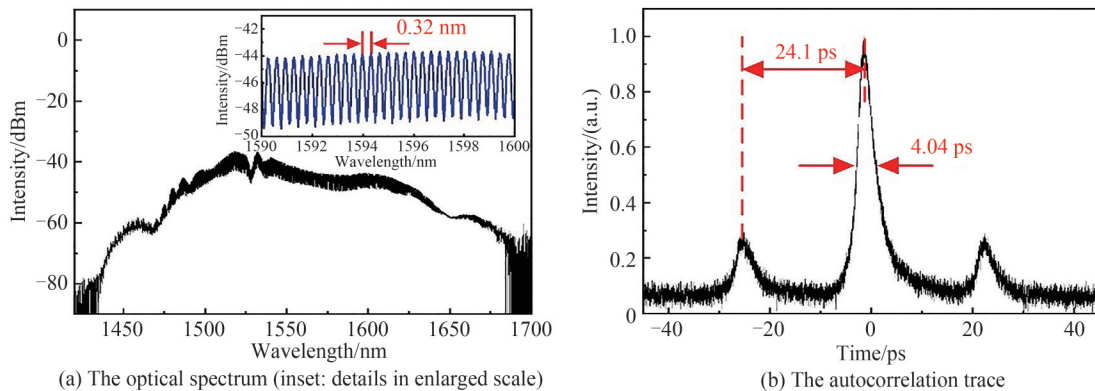


图7 色散管理孤子分子的输出特性

Fig.7 Output characteristics of the dispersion-managed soliton molecules

3 结论

在基于多模干涉效应锁模的光纤激光器中研究了展宽脉冲和色散管理孤子分子的输出特性。按照纤芯中心对齐的方式将GIMF熔接在两段SMF之间,并将GIMF内置在PC中,通过旋转挤压PC来改变多模光纤中脉冲光的相位,引入额外的相位差放宽SMS锁模结构对GIMF长度的限制,从而实现锁模脉冲输出。将泵浦1和泵浦2的功率分别调节至95.1 mW和750 mW,获得中心波长为1528 nm的展宽脉冲,脉冲持续时间为973.2 fs,3 dB光谱带宽为37.2 nm。经过腔外色散补偿后,展宽脉冲的脉冲宽度被压缩至280.1 fs,对应的3 dB带宽为38.5 nm。进一步将泵浦2增加至856 mW,仔细调节PC腔内可输出色散管理孤子分子。整个激光器系统结构紧凑、输出稳定,由于在谐振腔中加入了GIMF,实验获得的光纤激光器结构具有更高的损伤阈值,在光通信和材料加工等领域具有潜在的应用价值。

参考文献

- [1] NAZEMOSAADAT E, MAFI A. Nonlinear multimodal interference and saturable absorption using a short graded-index multimode optical fiber[J]. Journal of the Optical Society of America B, 2013, 30(5): 1357-1367.
- [2] LI H, WANG Z, LI C, et al. Self-starting mode-locked Tm-doped fiber laser using a hybrid structure of no core-graded index multimode fiber as the saturable absorber[J]. Optics & Laser Technology, 2019, 113: 317-321.
- [3] LI H, HU F, TIAN Y, et al. Continuously wavelength-tunable mode-locked Tm fiber laser using stretched SMF-GIMF-SMF structure as both saturable absorber and filter[J]. Optics Express, 2019, 27(10): 14437-14446.
- [4] WANG Z, WANG DN, YANG F, et al. Er-doped mode-locked fiber laser with a hybrid structure of a step-index-graded-index multimode fiber as the saturable absorber[J]. Journal of Lightwave Technology, 2017, 35(24): 5280-5285.
- [5] TEGIN U, ORTAC B. All-fiber all-normal-dispersion femtosecond laser with a nonlinear multimodal interference-based saturable absorber[J]. Optics Letters, 2018, 43(7): 1611-1614.

- [6] WANG Z, LI L, WANG DN, et al. Generation of pulse-width controllable dissipative solitons and bound solitons by using an all fiber saturable absorber[J]. Optics Letters, 2019, 44(3): 570-573.
- [7] THULASI S, SIVABALAN S. All-fiber femtosecond mode-locked Yb-laser with few-mode fiber as a saturable absorber[J]. IEEE Photonics Technology Letters, 2021, 33(5): 223-226.
- [8] DONG Z, LIN J, LI H, et al. Generation of mode-locked square-shaped and chair-like pulse based on reverse saturable absorption effect of nonlinear multimode interference[J]. Optics Express, 2019, 27(20): 27610-27617.
- [9] SHI G, FU S, SHENG Q, et al. Dual-wavelength noise-like pulse generation in passively mode-locked all-fiber laser based on MMI effect[C]. Fiber Lasers XV: Technology and Systems. International Society for Optics and Photonics, 2018, 10512: 105122B.
- [10] ZHANG Le, GUO Yubin, SUN Tiegang, et al. Switchable quadruple-wavelength fiber laser based on multimode interference filter and birefringent filter[J]. Acta Photonica Sinica, 2016, 45(2): 0206001.
张乐,郭玉彬,孙铁刚,等.基于多模干涉滤波器和双折射滤波器的四波长可开关光纤激光器[J].光子学报,2016,45(2): 0206001.
- [11] ILDAY F Ö, WISE F W, SOSNOWSKI T. High-energy femtosecond stretched-pulse fiber laser with a nonlinear optical loop mirror[J]. Optics Letters, 2002, 27(17): 1531-1533.
- [12] SUN Z, HASAN T, WANG F, et al. Ultrafast stretched-pulse fiber laser mode-locked by carbon nanotubes[J]. Nano Research, 2010, 3(6): 404-411.
- [13] ZHAO F, WANG Y, WANG H, et al. Ultrafast soliton and stretched-pulse switchable mode-locked fiber laser with hybrid structure of multimode fiber based saturable absorber[J]. Scientific Reports, 2018, 8(1): 1-7.
- [14] CHEN G, LI W, WANG G, et al. Generation of coexisting high-energy pulses in a mode-locked all-fiber laser with a nonlinear multimodal interference technique[J]. Photonics Research, 2019, 7(2): 187-192.
- [15] WANG Yishan, ZHAO Fengyan, WANG Hushan, et al. Research status and development of graded-index multimode fiber mode-locking technique (invited)[J]. Acta Photonica Sinica, 2020, 49(11): 1149003.
王屹山,赵凤艳,王虎山,等.渐变折射率多模光纤锁模技术的研究现状与展望(特邀)[J].光子学报,2020,49(11): 1149003.
- [16] LI H, WANG Z, LI C, et al. Mode-locked Tm fiber laser using SMF-SIMF-GIMF-SMF fiber structure as a saturable absorber[J]. Optics Express, 2017, 25(22): 26546-26553.
- [17] ZHAO F, WANG Y, WANG H, et al. High-energy solitons generation with a nonlinear multimode interference-based saturable absorber[J]. Laser Physics, 2018, 28(8): 085104.
- [18] MAFI A. Pulse propagation in a short nonlinear graded-index multimode optical fiber [J]. Journal of Lightwave Technology, 2012, 30(17): 2803-2811.
- [19] WANG Z, WANG DN, YANG F, et al. Stretched graded-index multimode optical fiber as a saturable absorber for erbium-doped fiber laser mode locking[J]. Optics Letters, 2018, 43(9): 2078-2081.
- [20] WANG T, JIN L, ZHANG H, et al. Gigahertz harmonic mode-locked fiber laser based on tunable SMS ultrafast optical switch[J]. Annalen der Physik, 2020, 532(5): 2000018.
- [21] ZHANG H, JIN L, ZHANG H, et al. All-fiber nonlinear optical switch based on polarization controller coiled SMF-GIMF-SMF for ultrashort pulse generation[J]. Optics Communications, 2019, 452: 7-11.
- [22] ZHANG H, JIN L, XU Y, et al. C-band wavelength tunable mode-locking fiber laser based on CD-SMS structure[J]. Applied Optics, 2019, 58(21): 5788-5793.
- [23] XU Xiang, JIANG Man, CHEN Haowei, et al. The Preparation of graphene based broadband saturable absorber and its application in laser[J]. Acta Photonica Sinica, 2014, 43(9): 99-103.
徐翔,江曼,李雕,等.基于石墨烯的宽带可饱和吸收体的制备及其在激光器中的应用[J].光子学报,2014,43(9): 99-103.
- [24] ZOU Baoying, DAI Jianan HONG Weiyi. Study on supercontinuum generation of femtosecond double pulses bound-state in optical fiber[J]. Chinese Journal of Lasers, 2020, 47(7): 0706003.
邹宝英,戴佳男,洪伟毅.光纤中飞秒双脉冲束束缚态产生超连续谱的研究[J].中国激光,2020,47(7): 0706003.
- [25] TANG D Y, ZHAO LM, ZHAO B, et al. Mechanism of multi-soliton formation and soliton energy quantization in passively mode-locked fiber lasers[J]. Physical Review A, 2005, 72(4): 043816.
- [26] LUO Y, XIANG Y, LIU B, et al. Dispersion-managed soliton molecules in a near zero-dispersion fiber laser[J]. IEEE Photonics Journal, 2018, 10(6): 1-10.
- [27] WANG Kaijie, WANG Hang, DU Tuanjie, et al. Effect of intracavity filtering bandwidth on bound-state soliton generation in normal dispersion regime[J]. Chinese Journal of Lasers, 2019, 46(8): 0806004.
王凯杰,王航,杜团结,等.腔内滤波带宽对正色散束缚态孤子形成的影响[J].中国激光,2019,46(8): 0806004.
- [28] ZHU T, WANG Z, WANG DN, et al. Observation of controllable tightly and loosely bound solitons with an all-fiber saturable absorber[J]. Photonics Research, 2019, 7(1): 61-68.

Generation of Stretched Pulse with Hundred-femtosecond Pulse Widths Based on Multimode-fiber Interference Effect

SUN Mengru^{1,2}, JI Haiying^{1,2}, XIONG Hao^{1,2}, HONG Yao¹, MA Wanzhuo^{1,2},
WANG Tianshu^{1,2}

(1 National and Local Joint Engineering Research Center of Space Optoelectronics Technology, Changchun
University of Science and Technology, Jilin 130022, China)

(2 College of Optoelectronics, Changchun University of Science and Technology, Jilin 130022, China)

Abstract: Ultrashort pulse fiber lasers have received widespread attention because they play a vital role in telecommunications, biology, and photonics. Many mode-locking technologies have been applied to construct passive mode-locking fiber lasers, such as semiconductor saturable absorption mirrors, graphene, nonlinear polarization rotation, carbon nanotubes, etc. In recent years, researchers have conducted extensive research on multimode fibers and proposed nonlinear multimode interference technology based on multimode fibers for the generation of ultrashort pulses. Compared with traditional mode-locked devices, multi-mode interference-based mode-locked devices have the advantages of high damage threshold, simple structure, adjustable wavelength and controllable modulation depth. In this study, we constructed a multimode interference mode-locked fiber laser by squeezing a piece of GIMF into the polarization controller works as SA. By introducing the dispersion management into the cavity, stretched pulse with 3 dB bandwidth of 37.2 nm was obtained. After compression, these pulses have a hundred-femtosecond duration. By carefully adjusting the PC and increasing the pump power, dispersion-managed soliton molecules was acquired, and the modulation period of spectrum is 0.32 nm. The experimental setup of the dispersion-managed all-fiber laser based on the SMS structure is depicted in Fig. 1. A 0.8 m long piece of single-mode HEDF was utilized as the gain medium, which was pumped by two 980 nm LDs through 980/1 550 nm WDM. Unidirectional operation was ensured by polarization independent optical isolator. The SA based on the SMS structure in the cavity was used as a mode-locking device, in which a 0.153 m long piece of GIMF was squeezed in the PC and the polarization states of the light in the multimode fiber was changed by tuning the PC. The net cavity dispersion can be managed by using a segment of DCF. In the experiment, the length of DCF is 0.3 m. The GVDs of HEDF, SMF, and DCF at 1.5 μm are 15.7, 18, and -152.6 ps/nm \cdot km, respectively. Due to the short length of the GIMF, the dispersion effect of the GIMF was neglected. Thus, the total net cavity dispersion is calculated to be -0.105 09 ps², and the laser operated in negative dispersion region. Considering the pigtails of all intracavity devices, the cavity length is 7.4 m, corresponding to the fundamental repetition frequency of 27.02 MHz. A 10:90 OC was employed to collect 10% power from the cavity. A compressed structure was built to acquire the minimum pulse width. In order to avoid the splitting and distortion of the pulse caused by the excessive peak power during the power amplification process, a section of DCF was welded between the PC and the amplifier to stretch the pulse in advance. As the gain medium of the amplifying structure, the EDF with normal dispersion at 1 550 nm was also used as a part of dispersion compensation. The dispersion caused by the amplifier further reduced the chirp of the pulse. When the pump 1 and pump 2 increased to 95.1 mW and 350 mW, self-starting dispersion-managed mode-locked pulse can be observed by appropriately rotating and squeezing the GIMF inside the PC. Figure 3 shows the features of the SP with pump 1 and pump 2 power of 95.1 mW and 750 mW. As the pump power increased, the spectral bandwidth and output power became wider and bigger and arrived its maximum of 37.2 nm and 1.7 mW respectively. Optimizing the length of DCF can compress the pulse from 973.2 fs to 280.1fs with the compressed structure after the output port of cavity. When the pump 2 increased to 856 mW, the pulses form stable soliton molecules by carefully adjusting the PC. The pulse width of a single dispersion-managed soliton molecules is 4.04 ps, and the pulse interval is 24.1 ps, which corresponds to the 0.32 nm spectral modulation period. The output characteristics of stretched pulses and dispersion-managed soliton molecules in dispersion-managed multimode interference mode-locked fiber lasers are studied. The output of the mode-locked pulse is realized by squeezing the graded index multimode fiber into the polarization controller. When the total pump power is 845.1 mW, a stretched pulse with a central wavelength of 1 528 nm, a 3 dB bandwidth of 37.2 nm and a pulse width of 973.2 fs is obtained by carefully adjusting the PC. A compressor is built to acquire the minimum pulse width and the DCF is used for dispersion

compensation to compress the pulse width of the stretched pulse to 280.1 fs. By further increasing the total pump power to 951.1 mW and adjusting the PC, the soliton molecules are obtained, and the modulation period of the dispersion-managed soliton molecules is 0.32 nm, corresponding to pulse interval of 24.1 ps. This phenomenon provides a reference for the research on multimode interference fiber lasers.

Key words: Fiber laser; Near-infrared; Multimode interference; Stretched pulse; Dispersion-managed soliton molecules

OCIS Codes: 140.4050; 320.5520; 320.7090